Numerical Simulation and Performance Analysis of a Water-Based Photovoltaic/Thermal (PVT) Collector Using Simulink Environment

Taoufik Brahim[1,2,*] and Abdelmajid Jemni[2]

[1]*University of Sousse, Higher Institute of Applied Sciences and Technology of Sousse (ISSATs), Laboratory of Study of Thermal and Energy Systems (LESTE- ENIM-Tunisia)*

[2]*University of Monastir, National Engineering School of Monastir, Laboratory of Study of Thermal and Energy Systems (LESTE- ENIM-Tunisia)*

Abstract: The hybrid photovoltaic-thermal (PVT) collector is an innovative technology that exploits solar energy to simultaneously generate electricity and heat. It thus optimizes the use of the surface exposed to sunlight by maximizing total energy production, offering a higher overall efficiency compared to standard thermal collectors or separately installed photovoltaic panels. In this research, a “sheet and tube” type water-based PVT collector was studied numerically. The main objective is to develop and analyze a hybrid PVT collector to optimize its overall efficiency. A mathematical model was developed for each component of the PVT collector (glass cover, PV module, absorber plate, tube, fluid, and insulation). Subsequently, the Hottel-Whillier thermal model was implemented and simulated in the Simulink/Matlab environment to study the collector’s performance. Furthermore, the effects of mass flow rate, number of glazings, inlet fluid temperature, and the heat transfer coefficient between the absorber plate and the PV module, among other operating parameters, were analyzed to identify their influence on electrical and thermal performance. A comparative analysis between PV and PVT collectors was conducted, and annual thermal and electrical energy productions were evaluated to assess the overall performance of each system.

Keywords: PVT, Simulink, Modeling, Performance.

1. INTRODUCTION

One of the major global challenges is to limit the use of fossil fuels, whose combustion generates significant greenhouse gas emissions contributing to climate change, while also being characterized by high price volatility. In this context, it is essential to develop and integrate renewable energy sources. Solar energy, in particular, is attracting increasing attention worldwide. Its exploitation, whether thermal or photovoltaic, requires the integration of different technologies depending on the mode of use.

Thermal solar energy employs various types of solar collectors that act as heat exchangers by absorbing solar radiation and converting it into thermal energy. This energy is then used to heat liquids such as water, for building heating and various industrial processes. Among the different collector categories are flat plate collectors, evacuated tubes, and concentrating collectors [1].

Photovoltaic energy involves panels or cells that intercept photons from the sun and convert them into electric current via the photoelectric effect. A large portion of the solar radiation captured by photovoltaic cells is not converted into electricity, leading to a temperature rise and a consequent decrease in performance. Moreover, when this temperature exceeds a certain threshold, it can cause progressive degradation of the cells over time [2, 3].

In this context, the temperature rise of PV collectors is a factor limiting their maximum efficiency. Therefore, sustained efforts are being made to limit overheating of photovoltaic modules while optimizing the recovery of the thermal energy they produce.

Hybrid PVT collectors represent a high-performance solution compared to the separate installation of thermal and photovoltaic collectors. By integrating both technologies into a single system, they fulfill a dual function: producing electricity from solar energy while recovering the heat usually dissipated. Recent research has explored various PVT configurations. Brahim and Jemni [4, 5] demonstrated that PVT systems with heat pipes achieve global efficiencies exceeding 56%. Lebbi *et al*. [6] experimentally validated a hybrid cooling system combining water spray and airflow, significantly enhancing electrical output. Othman *et al*. [7] reported a thermal efficiency of 76% for a dual-pass PVT system. Chaouch and *et al.* [8] analysis energy and exergy analysis of PVT solar collector using a long-term nonlinear dynamic roll bond PVT solar collector model. Advanced techniques such as jet impingement cooling have yielded thermal efficiencies up to 72% [9], while thermoelectric integration has increased electrical efficiency by 30% [10].

*Address correspondence to this author at the University of Sousse, Higher Institute of Applied Sciences and Technology of Sousse (ISSATs), Laboratory of Study of Thermal and Energy Systems (LESTE- ENIM-Tunisia);
E-mail: taoufik.brahim@yahoo.fr; taoufik.brahim@issatso.rnu.tn

Received on 15-11-2025 Accepted on 17-12-2025 Published on 21-12-2025

E-ISSN: 2410-2199/25

Nanofluids and phase change materials (PCMs) have also been investigated to enhance heat transfer. Hosseinzadeh *et al*. [11] achieved a global efficiency of 65.71% using PCM, and Preet *et al*. [12] reported a 12.6% increase in electrical efficiency with PCM integration. Simón-Allué *et al*. [13] observed a 26% improvement in thermal efficiency with PCM. Nanofluid-based systems have shown thermal efficiency gains up to 79.97% [14], though often at the cost of reduced electrical output due to optical losses.

the implementation of a dynamic, full-year (8760-hour) thermal–electrical simulation of a conventional sheet-and-tube PVT collector under real Tunisian weather conditions using the Simulink/MATLAB environment, a methodology rarely applied in prior studies on this widely deployable PVT configuration.

"The specific objectives of this study are:

(i) to develop a transient numerical model of a water-based sheet-and-tube PVT collector in Simulink/MATLAB.

(ii) to quantify the annual electrical and thermal energy gains of PVT over standalone PV under Tunisian climate (36°48′N, 10°10′E);

(iii) to determine optimal operating parameters, including mass flow rate (0.0003–0.3 kg/s), tube spacing (0.1–0.4 m), and glazing number (1–3);

(iv) to evaluate the techno-economic relevance of thermal recovery for residential applications in Mediterranean climates.

2. MATHEMATICAL MODEL

2.1. System Description

The studied PVT collector is of the “sheet and tube” water type. Solar radiation passes through the glass cover and reaches the photovoltaic module. A fraction of the incident solar irradiation is converted into electricity via the photovoltaic effect, while the remainder is conducted to the absorber plate. This heat is then transferred to the tubes welded to the absorber, which convey it by convection to the circulating heat-transfer fluid. Thermal insulation is placed on the rear face to minimize heat losses (Figure **1**). The PVT solar geometrical and electrical are given in Table **1** and Table **2** the assumptions in the model are:

1. Uniform irradiance over collector surface (valid for diffuse + beam on tilted plane).
2. Material properties constant.
3. Negligible thermal mass of glass and PV layers (quasi-steady thermal model per Hottel-Whillier).
4. Perfect contact between PV and absorber (represented via effective h_pv-abs).
5. 1D heat conduction through layers (standard for flat-plate collectors).

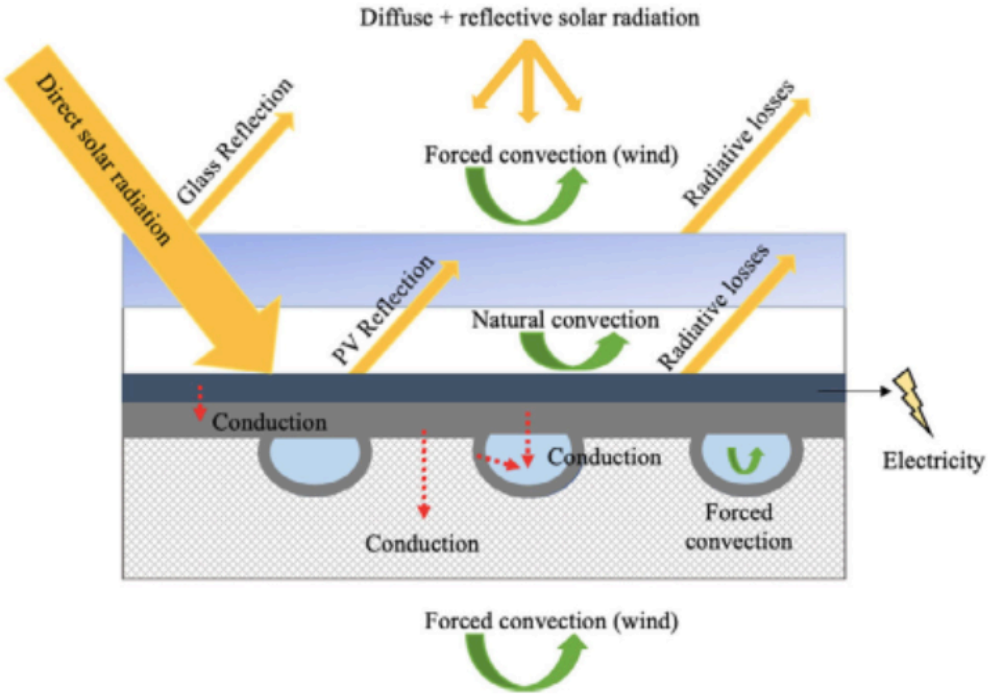

Figure 1: Schematic heat transfer processes in the layer of a PVT panel [16].

Table 1: Electrical Parameters of the PV Module

Parameter	Value
Maximum power (P_{max})	200 W
Voltage at maximum power point (V_{mp})	26.4 V
Current at maximum power point (I_{mp})	7.58 A
Open-circuit voltage (V_{oc})	32.9 V
Short-circuit current (I_{sc})	8.21 A
Total number of cells in series	54

Table .2: Characteristics of the PVT Collector Used in Simulation

Parameter	Symbol	Value	Unit
Collector surface area	A_c	1.32	m²
Number of glazings	—	1	—
Glass emissivity	ε_g	0.88	—
Absorber plate emissivity	ε_{abs}	0.95	—
Transmittance	τ	0.88	—
Absorptance	α	0.95	—
Fluid heat transfer coefficient	h_f	300	W/m²·K
Fluid specific heat capacity	$C_{p,f}$	4180	J/kg·K
PV panel thickness	δ_{pv}	0.04	m
PV thermal conductivity	k_{pv}	130	W/m·K
Absorber thickness	δ_{abs}	0.001	m
Absorber thermal conductivity	k_{abs}	390	W/m·K
Stefan-Boltzmann constant	σ	5.67×10^{-8}	W/m²·K⁴
Mass flow rate range	$\dot{m}$	0.0003–0.3	kg/s
Tube diameter	D	0.0097	m
Tube spacing	W	0.1	m
Collector tilt angle	—	45	°

2.2. Electrical Model

The electrical model of the PV module is based on the single-diode model. The output current of the solar cell is given by:

$$I = I_{ph} - I_0\left[\exp\left(\frac{q(V+IR_S)}{nkT}\right) - 1\right] \quad (1)$$

The photocurrent I_{ph} is proportional to solar irradiance:

$$I_{ph} = I_{sc,ref}\left(\frac{G_T}{G_{ref}}\right)\left[1 + \beta(T_{cell} - T_{ref})\right] \quad (2)$$

The electrical power is:

$$\dot{Q}_{el} = VI \quad (3)$$

Electrical efficiency is expressed as [17]:

$$\eta_{el} = \eta_{ref}\left[1 - \beta(T_{cell} - T_{ref})\right] \quad (4)$$

2.3. Thermal Model: Energy Balances and Hottel-Whillier Approach

In this section, the thermal model is detailed. The Hottel-Whillier model was selected to evaluate the performance of the PVT collector.

The useful thermal power as the enthalpy gain of the fluid, *i.e*., the net heat extracted by water flow is given by :

$$\dot{Q}_u = \dot{m}C_p(T_o - T_i) \quad (5)$$

where

$\dot{m}$ is the mass flow rate of water,

C_p is the specific heat capacity of the fluid,

T_o and T_i are the outlet and inlet fluid temperatures, respectively.

The useful thermal power $\dot{Q}_u$ is also expressed as the difference between the solar power absorbed by the absorber plate and the thermal losses [61]:

$$\dot{Q}_u = A_c\left[G(\tau\alpha)_{PV} - U_L(T_{pm} - T_a)\right] \quad (6)$$

where

A_c is the collector surface area,

G is the solar irradiance incident on the absorber,

$(\tau\alpha)_{PV}$ is the effective transmittance–absorptance product of the PV/glazing system,

U_L is the overall heat loss coefficient,

T_{pm} is the mean plate temperature,

T_a is the ambient temperature.

Eq. (6): Balances absorbed solar power against convective/radiative losses, central to flat-plate collector theory.

Since the calculation and measurement of T_{pm} are complex due to its dependence on absorber characteristics, the flat-plate collector equation according to Hottel-Whillier is simplified by replacing T_{pm} with the fluid inlet temperature T_i [18]:

$$\dot{Q}_u = A_cF_R[G(\tau\alpha)_{PV} - U_L(T_i - T_a)] \quad (7)$$

where F_R is the heat removal factor, defined as:

$$F_R = \frac{\dot{m}C_p}{A_c U_L}\left[1 - \exp\left(-\frac{A_c U_L F'}{\dot{m}C_p}\right)\right] \quad (8)$$

The heat removal factor FRFR quantifies how effectively fluid removes heat compared to ideal performance; it depends on flow rate, tube geometry, and interfacial heat transfer.

and F' is the collector efficiency factor, given by:

$$F' = \frac{1}{U_t} / \left[\frac{1}{w}\left(\frac{1}{U_t(D+(W-D)F)} + \frac{1}{wh_{pv}} + \frac{1}{\pi D h_{fi}}\right)\right] \quad (9)$$

In this expression:

W is the tube spacing,

D is the tube diameter,

h_{pv} is the heat transfer coefficient at the PV–absorber interface,

h_{fi} is the internal fluid heat transfer coefficient,

F is the fin efficiency factor.

The fin efficiency F is calculated as:

$$F = \frac{\tanh\left(M\frac{(W-D)}{2}\right)}{M\frac{(W-D)}{2}} \quad (10)$$

where M represents the combined thermal conductance of the PV module and absorber plate [19]

$$M = \sqrt{\frac{U_L}{k_{abs}\cdot l_{abs} + k_{pv}\cdot l_{pv}}} \quad (11)$$

with:

k_{abs}, l_{abs}: thermal conductivity and thickness of the absorber,

k_{pv}, l_{pv}: thermal conductivity and thickness of the PV module.

The overall heat loss coefficient U_L is defined as [50]:

$$U_L = U_e + U_t + U_b \quad (12)$$

where:

U_t: top heat loss coefficient,

U_b: bottom heat loss coefficient,

U_e: edge (lateral) heat loss coefficient.

The top loss coefficient U_t is given by [21]:

$$U_t = \left\{\frac{N}{\frac{C}{T_{pm}}\left[\frac{T_{pm}-T_a}{(N+f)}\right]^e} + \frac{1}{h_w}\right\}^{-1} + \frac{\sigma(T_{pm}+T_a)(T_{pm}^2+T_a^2)}{\left(\varepsilon_p+0.00591Nh_w\right)^{-1}+\frac{2N+f-1+0.133\varepsilon_p}{\varepsilon_g}-N} \quad (13)$$

The bottom loss coefficient is:

$$U_b = \frac{k_b}{L_b} = \frac{k_e A_e}{L_e A_c} \quad (14)$$

The wind convection coefficient is:

$$h_w = 5.7 + 3.8V \quad (15)$$

where V is wind speed (m/s).

The mean plate temperature is iteratively estimated as:

$$T_{pm} = T_i + \frac{\dot{Q}_u/A_c}{F_R U_t} \quad (16)$$

Additional empirical parameters are:

$$f = \left(1 + 0.089h_w - 0.01166h_w\varepsilon_p\right)(1 + 0.07866N) \quad (17)$$

$$C = 520(1 - 0.00005\beta^2) \quad (18)$$

$$e = 0.43\left(1 - \frac{100}{T_{pm}}\right) \quad (19)$$

Finally, the thermal and electrical efficiencies are given by [22]:

$$\eta_{th} = F_R\left[(\tau\alpha)_{PV} - \frac{U_L(T_i - T_a)}{G}\right] \quad (20)$$

$$\eta_{el} = 0.15\left[1 - 0.0045(T_{pm} - 25)\right] \quad (21)$$

Where;

ε_p: absorber plate emissivity. ε_g: glass emissivity .σ: Stefan–Boltzmann constant (5.67×10^{-8}W/m$^2\cdot$K^4). N: number of glazings. β: collector tilt angle (degrees) and h_w: convective heat transfer coefficient due to wind

The complete system was modeled in Simulink/Matlab (Figure **2**).

Hourly meteorological data for Tunis (2023) were obtained from the NASA POWER database; including global horizontal irradiance (GHI), ambient temperature, and wind speed at 1-hour resolution. GHI was converted to plane-of-array irradiance using the isotropic sky model. All simulations used hourly time steps over 8760 hours (full year). Ambient temperature and wind speed profiles directly modulated top heat loss coefficient U_t via Eq. (15).

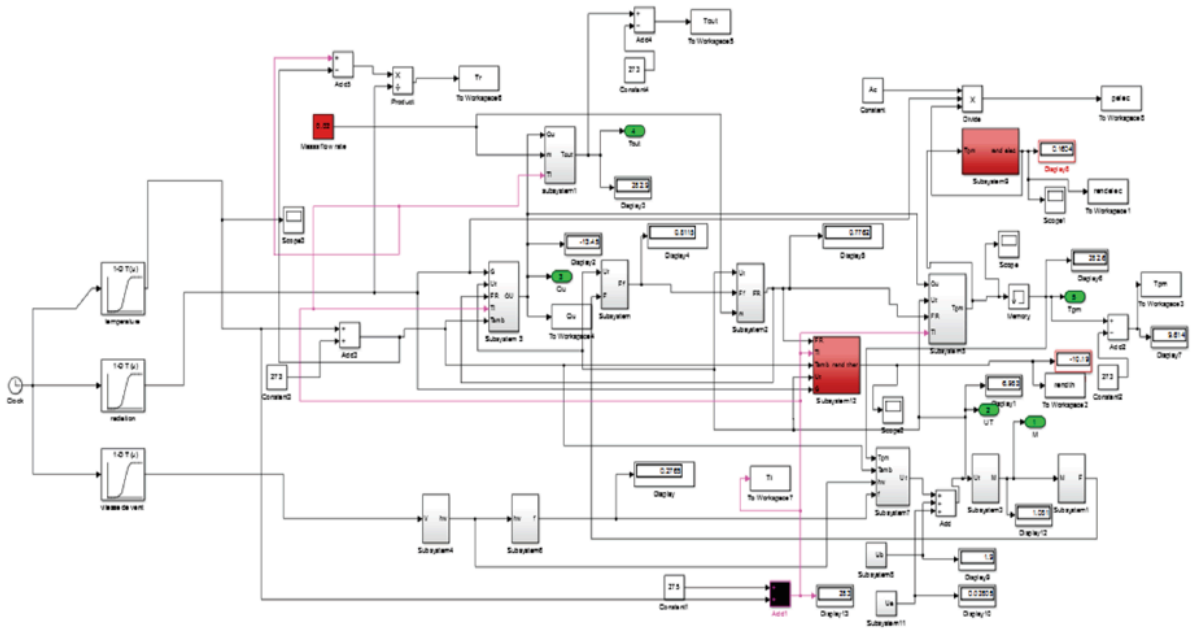

Figure 2: Graphical illustration of simulation model.

3. RESULTS AND DISCUSSION

Simulations were performed over 8760 hours using meteorological data from Tunis (36°48′N, 10°10′E). Figure **3** reports a comparative study of the daily electrical production of PV and PVT collectors, simulated for two typical days, January 22 (winter) and August 15 (summer), considering a flow rate of 0.02 kg/s. It can be seen that the PVT collector generates a higher electrical production than the PV collector, with a particularly marked difference during peak sunshine, between 11:00 and 14:00. During the day of January 22, the average electrical power produced by the PV collector is 25.11 W, with a maximum of 107.19 W, while the PVT collector reaches an average of 25.54 W and a maximum of 109.45 W, representing a gain of 1.69%. In summer, on August 15, the average daily values were 39.41 W for PV (maximum of 132.49 W) and 40.21 W for PVT (maximum of 135.77 W), representing a 2.47% improvement compared to a PV collector. This improvement is explained by the efficiency of the heat transfer fluid in cooling the photovoltaic cells, particularly in summer when overheating is more significant. This helps reduce the efficiency loss caused by this overheating.

Although the PVT system improves electricity production in winter, this gain remains relatively small due to low ambient temperatures and strong wind-induced convection, which ensures natural cooling of the photovoltaic cells. The benefits of the PVT system are more evident in summer, when solar irradiation is high. This confirms that the thermal coupling of PVT collectors is particularly suitable for hot, sunny regions. This comparison highlights the potential energy benefits linked to the integration of thermal recovery in a PVT system.

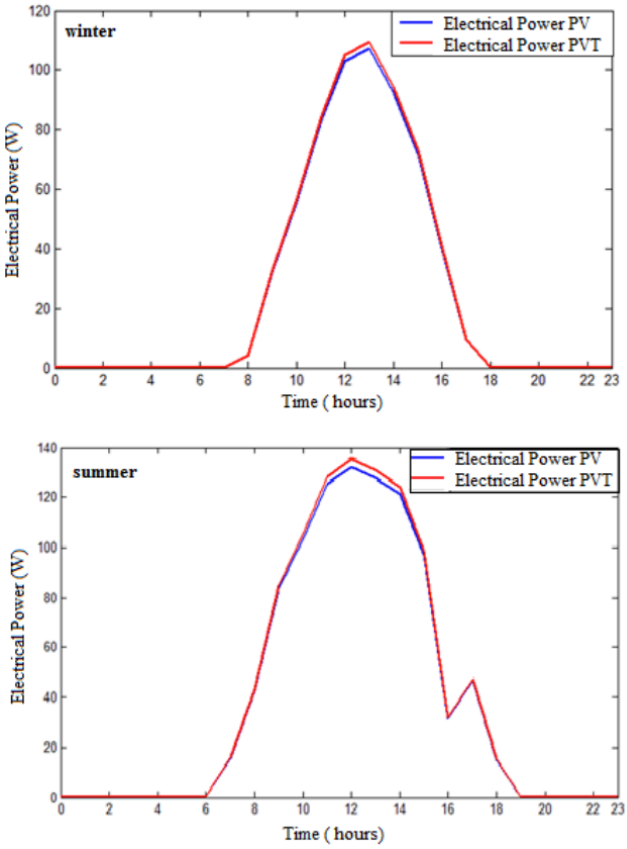

Figure 3: Comparative study of daily electricity production.

The evolution of cell temperature, thermal efficiency, and useful thermal energy for fluid flow rates ranging from 0.0003 kg/s to 0.3 kg/s is illustrated in Figure **4**. For the lowest flow rate of 0.0003 kg/s, the average cell temperature is 17.14°C, with a maximum peak of

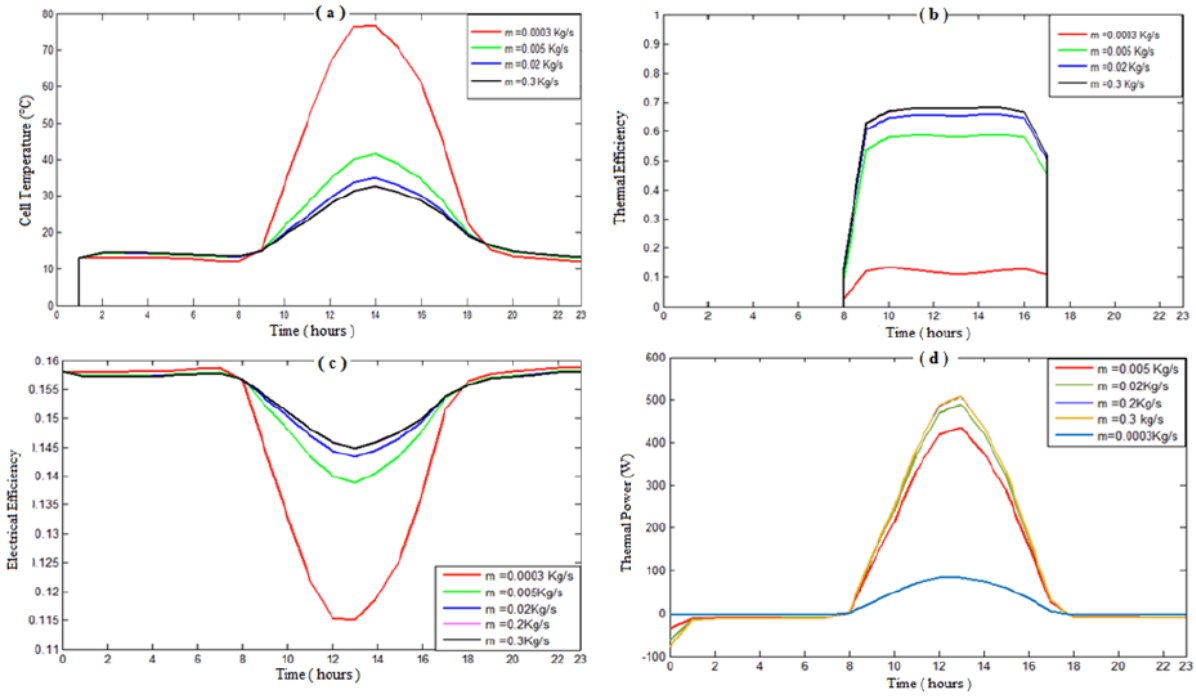

Figure 4: Effect of fluid flow on electrical and thermal outputs

76.81°C. The average useful energy is 19.07 W (maximum 84.13 W), while the thermal efficiency reaches a maximum of 13%. In comparison, at a flow rate of 0.3 kg/s, the average temperature drops to 6.81°C (maximum = 32.67°C), the average useful energy rises to 104.4 W (maximum = 508.32 W), and the thermal efficiency reaches 68.12%. These results reveal that increasing the flow rate significantly improves the thermal performance of the collector, the average cell temperature decreases by about 60.3%, the thermal efficiency increases by 13% to 68.21%, and the average useful heat is increased by more than six times.

Figure **4c** illustrates the influence of varying the heat transfer fluid flow rate on the average daily electrical efficiency, which increases from 14.7% to 15.4% when the flow rate changes from 0.0003 kg/s to 0.3 kg/s. These results demonstrate that increasing the flow rate improves the average daily electrical efficiency by approximately 4.7%. The 60% drop in cell temperature with increasing flow rate aligns with Newton's law of cooling: higher $\dot{m}$ enhances convective heat removal, reducing PV junction temperature and mitigating the negative temperature coefficient (~−0.4%/°C for crystalline Si). This explains the 4.7% electrical efficiency gain.

The influence of wind speed on thermal and electrical power is presented in Figure **5**, revealing an improvement in electrical power of 1.47% in August and 0.417% in January. The observed variation is explained by seasonal thermal conditions. In summer (August), Even with relatively low wind speeds, its cooling effect is more significant due to the significant overheating of the photovoltaic cells, caused by high ambient temperatures and strong solar irradiation. In winter (January), the lower outdoor temperature already ensures partial cooling of the cells, which limits the additional impact of the wind, although it remains measurable. For thermal power, a decrease of 3.25% is observed in August, compared to a more pronounced drop of 11.4% in January when wind is present. This difference is explained by greater convective heat losses in winter, due to a greater temperature difference between the collector and the ambient air. In summer, although there is wind, the higher outside temperature reduces this thermal gradient, thus limiting losses. We can conclude that the impact of wind on thermal power is therefore significantly more significant in winter.

The effect of varying the tube spacing on the thermal and electrical performance of a PVT collector is shown in Figure **6**. By varying the tube spacing from 0.1 m to 0.4 m, we observed a slight decrease in the average electrical efficiency, from 15.39% to 15.26%, corresponding to a relative reduction of 0.844% (Figure **5.a**). However, the thermal efficiency decreases significantly, from 65.84% to 55.73%, corresponding to a loss of 13.03%. This decrease is explained by the fact that too large a spacing between the tubes prevents a large portion of the absorbing surface from being in direct contact with them. This reduces the efficiency of heat transfer between the plate and the heat transfer fluid. Consequently, heat accumulates in

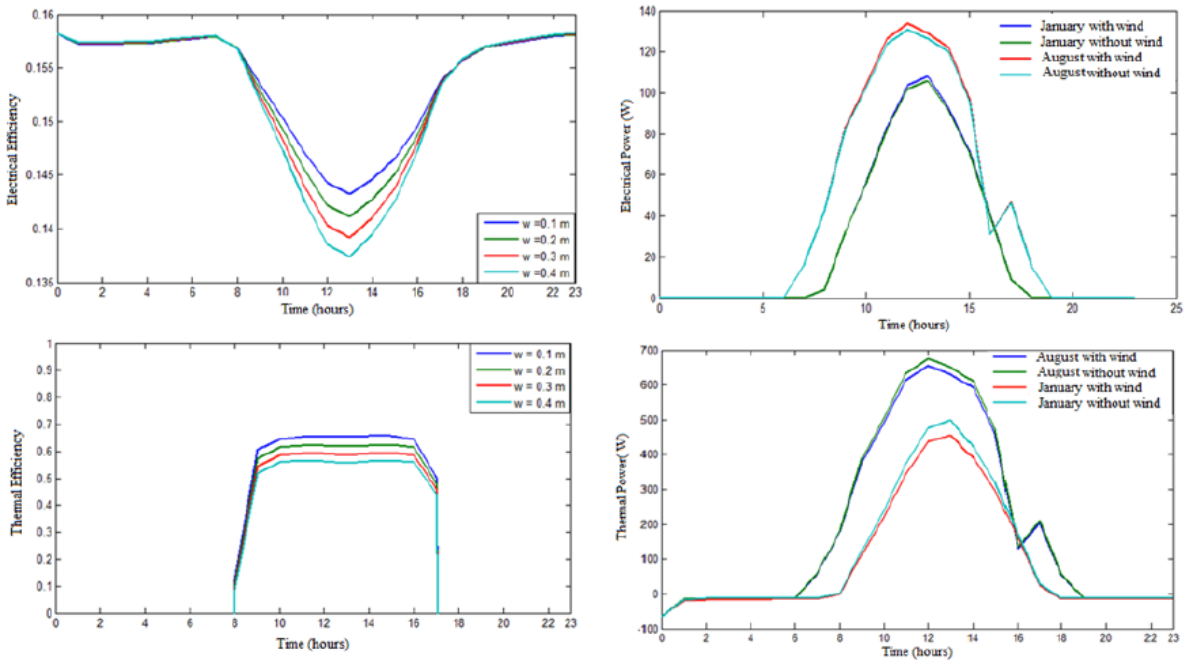

Figure.5: Effect of wind speed on electrical and thermal outputs.

the plate, raising its temperature. This overheating then leads to an increase in heat losses by convection and radiation to the environment.

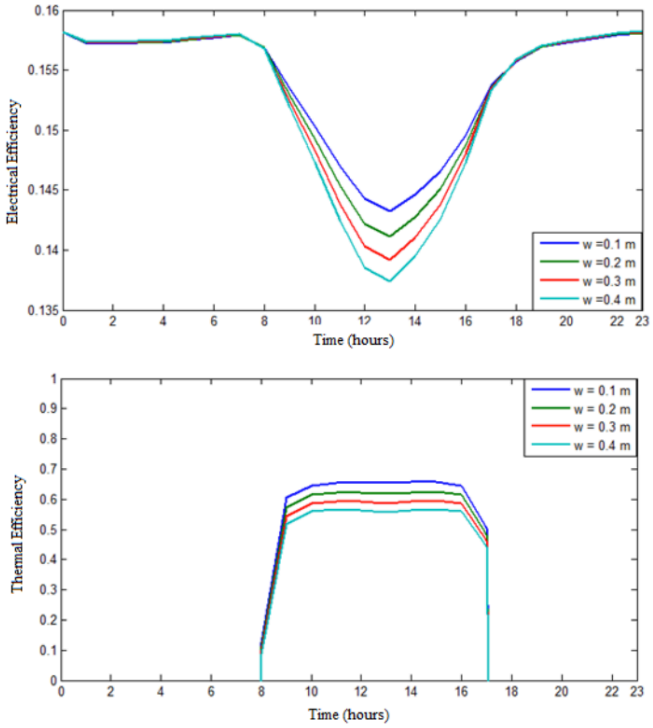

Figure 6: Effect of tube spacing on electrical and thermal outputs.

Figure **7** shows the effect of insulation on the daily thermal and electrical power outputs provided by the collector over the two simulation days with a mass flow rate of $\dot{m}$ = 0.02 kg/s. The data obtained reveal that the addition of insulation significantly improves thermal power, particularly during the winter period. In January, the average daily power increased from 91.27 W (maximum of 456.6 W) without insulation to 97.94 W (maximum of 489.7 W) with insulation, an increase of 6.81%. In August, it increased from 177.07 W (maximum of 655.09 W) to 187.54 W (maximum of 680.07 W), which corresponds to an improvement of 5.5%. A more significant improvement observed in

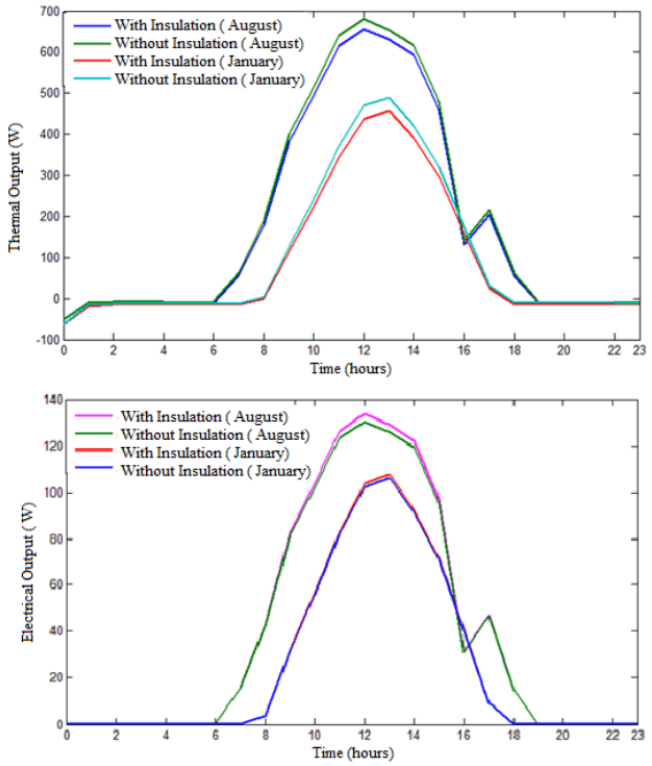

Figure 7: Effect of insulation on electrical and thermal outputs.

winter is explained by the fact that the addition of insulation limits heat loss by convection to the outside. In conditions of low sunlight and low ambient temperatures, it ensures better heat conservation at the absorber level, which results in a significant thermal gain. On the other hand, the addition of insulation leads to a decrease in electrical power: it decreases from 107.93 W to 106.23 W in January (a decrease of 1.18%) and from 133.6 W to 130.2 W in August (a reduction of 1.92%). This decrease is explained by the fact that the insulation reduces heat loss behind the collector, leading to an increase in heat within the photovoltaic cells, particularly in summer. The trade-off between thermal gain and electrical loss is a well-documented dilemma in PVT design [17, 20]. Our results confirm that while rear insulation suppresses conductive losses (U_b), it elevates PV temperature, highlighting the need for active cooling even in winter."

The increase in the number of glazings (as illustrated in Figure **8**) from 1 to 3 caused a 13.02% increase in the average daily thermal power, from 177.07 W to 200.12 W, while the electrical power decreased by 2.26%. This change is explained by the greenhouse effect created by the additional glazings, which promote the accumulation of heat inside the collector, thus increasing the internal temperature and improving thermal recovery by the heat transfer fluid.

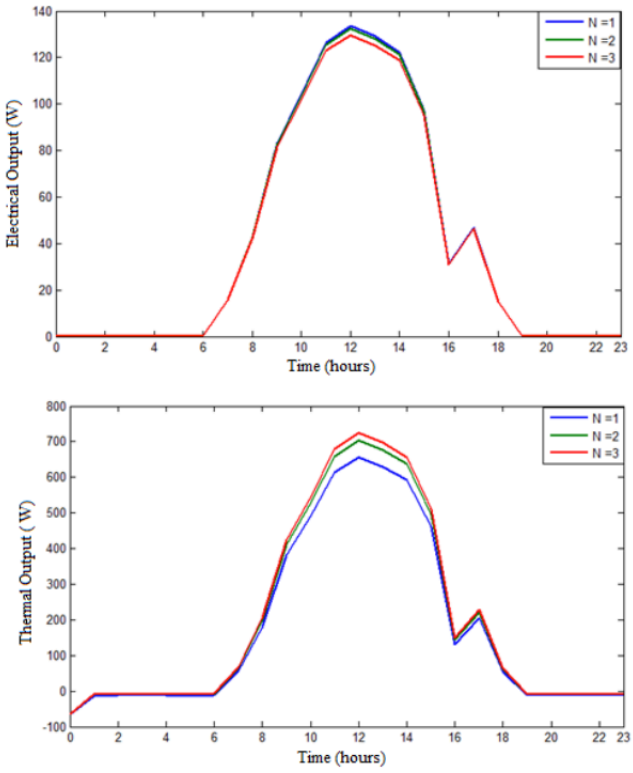

Figure 8: Effect of glass cover number on electrical and thermal outputs.

Figure **9** illustrates the influence of the heat transfer coefficient h_{PV} on electrical and thermal production. When the heat transfer coefficient increases from 45 to 100 W/m². K, the average daily thermal power increases from 177.07 W to 188.15 W, an improvement of 6.86%. This thermal improvement is also accompanied by a 1.94% increase in electrical power.

This increase is explained by the fact that a higher heat transfer coefficient h_{PV} promotes more efficient heat exchange between the photovoltaic cells and the heat transfer fluid, which increases heat recovery, thus contributing to better electrical performance.

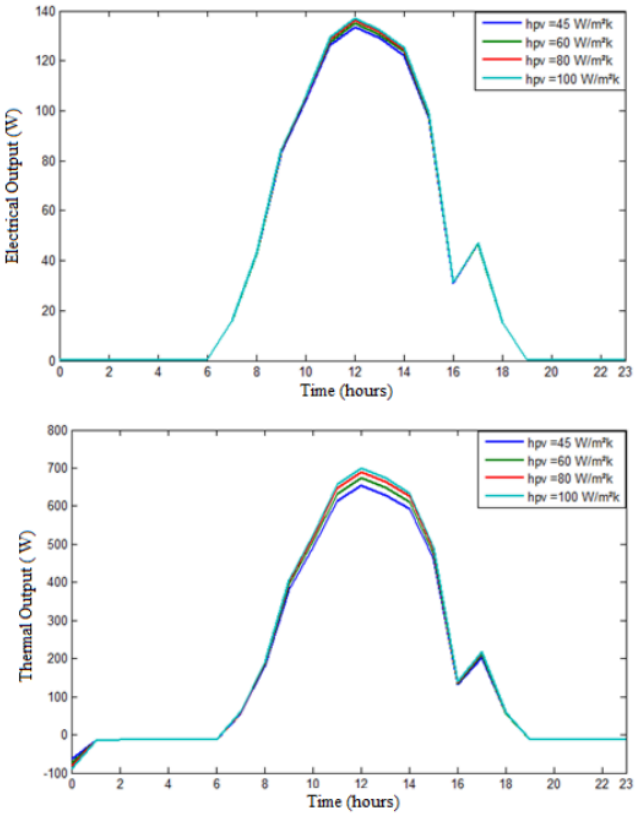

Figure 9: Effect of internal heat transfer coefficient on electrical and thermal outputs.

The annual electrical and thermal production for an optimal flow rate, m ̇=0.2kg/s is illustrated in Figure **10**. The average annual electrical production of PVT is 26.69 W with a more significant contribution during the period from March 15 to October 14. As for the average annual thermal power, it is around 114.43 W, with significant production observed between March 20 and September 15.

4. CONCLUSION

His study presents a comprehensive numerical investigation of a water-based “sheet-and-tube” photovoltaic/thermal (PVT) collector using the Hottel-Whillier thermal model implemented in Simulink/Matlab. The model was validated against experimental data from Brahim & Jemni [67], showing excellent agreement in both thermal and electrical

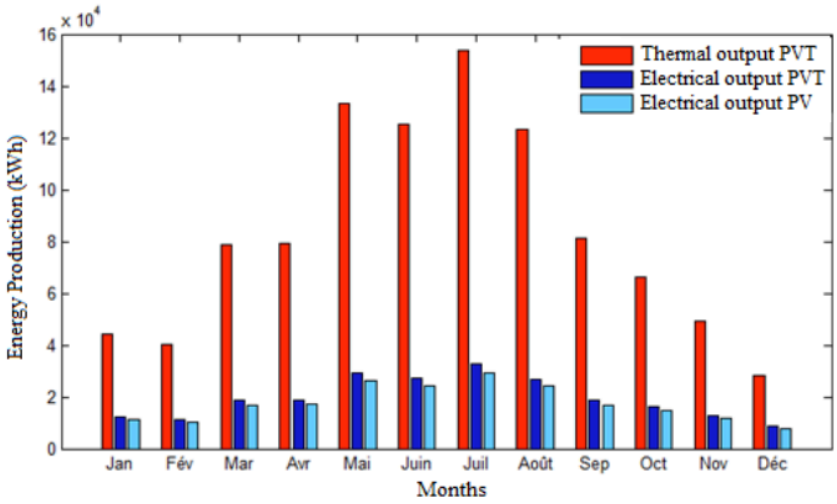

Figure 10: Annual energy production.

efficiency trends. The simulations, conducted over a full annual cycle (8760 h) under Tunisian climatic conditions, yielded the following key quantitative results:

- Electrical performance: The PVT system outperformed a conventional PV panel by 1.69% in winter (22 January) and 2.47% in summer (15 August), with annual electrical production of 233.86 kWh/m² versus 210 kWh/m² for standalone PV.
- Thermal performance: Annual thermal energy output reached 1002.47 kWh/m², with peak thermal efficiency of 71.2% in summer.
- Optimal mass flow rate: A flow rate of 0.2 kg/s was identified as optimal—beyond this, further increases yielded negligible cooling benefits. At this flow rate, thermal efficiency rose from 13% to 68.21%, and useful heat output increased sixfold.
- Adding insulation improved thermal power by 6.81% (winter) and 5.5% (summer) but reduced electrical output by 1.18–1.92% due to higher cell temperatures.
- Increasing glazing from 1 to 3 layers boosted thermal power by 13.02% but decreased electrical power by 2.26% (greenhouse effect).
- Enhancing the PV–absorber heat transfer coefficient (h_{PV}) from 45 to 100 W/m²·K increased both thermal (+6.86%) and electrical (+1.94%) outputs.
- Tube spacing beyond 0.1 m caused a 13.03% drop in thermal efficiency, highlighting the importance of compact absorber design.
- Seasonal behavior: Electrical efficiency peaked in winter (15.42%), while thermal efficiency was highest in summer (71.2%), confirming the PVT system's suitability for hot, sunny climates.

These results demonstrate that strategic optimization of operating and geometric parameters can significantly enhance the dual functionality of PVT collectors. The 23.8 kWh/m² annual electrical gain over conventional PV (233.85 kWh/m² for PVT, 210 kwh/m² for PV) combined with over 1000 kWh/m² of usable heat, underscores the technology's potential for residential and industrial applications in Mediterranean and arid regions.

This work not only validates the Hottel-Whillier model for dynamic PVT simulation but also provides actionable design guidelines for maximizing energy yield, contributing directly to the advancement of high-efficiency solar hybrid systems guidelines for optimizing PVT collector design and sizing under varying climatic conditions.

NOMENCLATURE

Latin Symbols

$\dot{Q}_g$: Solar power absorbed by the glass cover

$\dot{Q}_{th}$: Thermal power

$\dot{Q}_{el}$: Electrical power

$\dot{Q}_u$: Useful thermal power

U_L: Overall heat loss coefficient

G_T: Solar irradiance received by the collector

k: Thermal conductivity

C_p: Specific heat

h: Heat transfer coefficient

m: Mass

S: Surface area

P_i: Internal tube perimeter

D_i: Internal tube diameter

D_h: Hydraulic diameter

T: Temperature

I_0: Diode saturation current

I_{ph}: Photocurrent generated by incident light

V: Output voltage of the solar cell

q: Electron charge

β: Temperature coefficient

I_{sc}: Short-circuit current

n: Diode ideality factor

PF: Packing factor

F': Heat extraction factor

Greek Symbols

σ: Stefan-Boltzmann constant

δ: Thickness

ρ: Density

η_{el}: Electrical efficiency

η_{th}: Thermal efficiency

α: Absorptance

τ: Transmittance

ε_g: Emissivity of glass

ε_{pv}: Emissivity of PV panel

Subscripts

g: Glass

pv: Photovoltaic module

a: Air

i: Internal

eva: EVA layer

amb: Ambient

ref: Reference

u: Useful

r: Radiation

c: Convection

cond: Conduction

f: Fluid

t: Tube

abs: Absorber plate

el: Electrical

REFERENCES

[1] Taoufik, B., and Abdelmajid, J. (February 11, 2022). "Feasibility Study of Long-Term Dual Tank Photovoltaic/Thermal Indirect Parallel Solar-Assisted Heat Pump Systems." ASME. J. Sol. Energy Eng. August 2022; 144(4): 041006. https://doi.org/10.1115/1.4053317

[2] Saidi, S., Brahim, T., & Jemni, A. (2025). Experimental advances in photovoltaic-thermal (PVT) systems: a comprehensive review of cooling technologies, materials, and performance optimization. Solar Energy, 298, 113650. https://doi.org/10.1016/j.solener.2025.113650

[3] Saidi, S., Brahim, T., & Jemni, A. (2025). Numerical investigation of indirect parallel PVT solar systems using MATLAB/simulink. Engineering Research Express, 7(1), 015339. https://doi.org/10.1088/2631-8695/adae55

[4] Brahim, T. and Jemni, A. (2021b) “Parametric study of photovoltaic/thermal wickless heat pipe solar collector,” Energy conversion and management, 239(114236), p. 114236. https://doi.org/10.1016/j.enconman.2021.114236

[5] Brahim, T. and Jemni, A. (2015) “Numerical investigation of roll heat pipe type for heat exchangers thermal management,” Applied thermal engineering, 90, pp. 638-647. https://doi.org/10.1016/j.applthermaleng.2015.07.048

[6] Lebbi, M., *et al*. (2021). Energy performance improvement of a new hybrid PV/T Bi-fluid system using active cooling and self-cleaning: experimental study. Applied Thermal Engineering, 182, 116033. https://doi.org/10.1016/j.applthermaleng.2020.116033

[7] Othman, M. Y., *et al*. (2016). Performance analysis of PV/T Combined with water and air heating system: an experimental study. Renewable Energy, 86, 716-722. https://doi.org/10.1016/j.renene.2015.08.061

[8] Chaouch, A., Brahim, T., Abdelati, R., & Jemni, A. (2024). Energy and exergy analysis of a long-term nonlinear dynamic roll bond PVT solar collector model under Tunisian (North Africa) climatic conditions. Thermal Science and Engineering Progress, 53, 102727. https://doi.org/10.1016/j.tsep.2024.102727

[9] Hasan, H. A., Sopian, K., & Fudholi, A. (2018). Photovoltaic thermal solar water collector designed with a jet collision system. Energy, 161, 412-424. https://doi.org/10.1016/j.energy.2018.07.141

[10] Yang, D., & Yin, H. (2016). Energy Conversion Efficiency of a Novel Hybrid Solar System for Photovoltaic, Thermoelectric, and Heat Utilization. IEEE Transactions on Energy Conversion, 26(2), 662-670. https://doi.org/10.1109/TEC.2011.2112363

[11] Hosseinzadeh, M., *et al*. (2018). Energy and exergy analysis of nanofluid based photovoltaic thermal system integrated with phase change material. Energy, 147, 636-647. https://doi.org/10.1016/j.energy.2018.01.073

[12] S. Preet, B. Bhushan, T. Mahajan, Experimental investigation of water based photovoltaic/thermal (PV/T) system with and without phase change material (PCM), Sol. Energy 155 (2017) 1104-1120. https://doi.org/10.1016/j.solener.2017.07.040

[13] Simón-Allué, R., *et al*. (2022). Performance evaluation of PVT panel with phase change material: Experimental study in lab testing and field measurement. Solar Energy, 241, 738-751. https://doi.org/10.1016/j.solener.2022.05.035

[14] Rajaee, F., Rad, M. A. V., Kasaeian, A., Mahian, O., & Yan, W.M. (2020). Experimental analysis of a photovoltaic/thermoelectric generator using cobalt oxide nanofluid and phase change material heat sink. Energy Conversion and Management, 212, 112780. https://doi.org/10.1016/j.enconman.2020.112780

[15] Brahim, T., Abdelati, R., & Jemni, A. (2024). Dynamic simulation of roll bond PVT solar collector under Simulink/Matlab. Engineering Research Express, 6(4),

045340.
https://doi.org/10.1088/2631-8695/ad8ff5

[16] Barbu, M., Siroux, M., & Darie, G. (2021). Numerical model and parametric analysis of a liquid based hybrid photovoltaic thermal (PVT) collector. Energy Reports, 7, 7977-7988. https://doi.org/10.1016/j.egyr.2021.07.058

[17] Florschuetz, L. W. (1979). Extension of the Hottel-Whillier model to the analysis of combined photovoltaic/thermal flat plate collectors. Solar Energy, 22(4), 361-366. https://doi.org/10.1016/0038-092X(79)90190-7

[18] Duffie, J. A., Beckman, W. A., & Blair, N. (2020). Solar Engineering of Thermal Processes, Photovoltaics and Wind.

[19] Vokas, G., Christandonis, N., & Skittides, F. (2006). Hybrid photovoltaic-thermal systems for domestic heating and cooling—A theoretical approach. Solar Energy, 80(5), 607-615. https://doi.org/10.1016/j.solener.2005.03.011

[20] Tiwari, A., & Sodha, M. S. (2006). Performance evaluation of solar PV/T system: An experimental validation. Solar Energy, 80(7), 751-759. https://doi.org/10.1016/j.solener.2005.07.006

[21] Klein, S. A. (2018). Calculation of Flat-Plate Collector Loss Coefficients. Renewable Energy, 387-391. https://doi.org/10.4324/9781315793245-69

[22] Piratheepan, M., & Anderson, T. N. (2015). Natural convection heat transfers in façade integrated solar concentrators. Solar Energy, 122, 271-276. https://doi.org/10.1016/j.solener.2015.09.008

https://doi.org/10.31875/2410-2199.2025.12.12